JOURNAL OF GEOPHYSICAL RESEARCH, VOL. 100, NO. D8, PAGES 16,387–16,393, AUGUST 20, 1995

The effects of horizontally extended clouds on backscattered ultraviolet sunlight

Guoyong Wen and John E. Frederick

Department of the Geophysical Sciences, University of Chicago, Chicago, Illinois

Abstract. This work examines the effects of clouds on backscattered ultraviolet radiation via analysis of satellite observations and radiative transfer modeling. Measurements from the continuous scan mode of the Nimbus 7 SBUV instrument show that the enhancement in backscatter albedo associated with clouds generally increases with wavelength. However, high clouds enhance the backscattered ultraviolet radiation at short wavelengths more than do low or middle level clouds. For an overhead Sun in the tropics, the enhancements in backscattered radiance from high clouds are about 5 times those from low clouds at a wavelength of 300 nm. For a typical mid-latitude atmosphere with a solar zenith angle of 60°, the enhancements in backscattered radiance from high clouds are approximately double those due to low level clouds.

Introduction

Backscattering of ultraviolet (UV) sunlight into space by clouds is a significant factor in determining the climatology of biologically relevant radiation at the Earth's surface [*Frederick and Lubin*, 1988]. This backscattered light was routinely observed by the solar backscattered ultraviolet (SBUV) spectral radiometer carried on the Nimbus 7 satellite. A valuable long-term objective would be to utilize backscattered radiances measured from satellites to infer both the ozone amount and the reflecting properties of clouds in the UV. One could then use this information to estimate the solar spectral irradiance reaching the Earth's surface on a global scale for use in studies of photobiology and atmospheric chemistry. The analysis reported here represents a first step toward this objective by examining the effects of clouds on backscattered UV radiation.

The SBUV continuous scan measurements, with their high spectral resolution, are useful for inferring the ozone amount in the atmosphere [*Wen and Frederick*, 1994]. In the presence of clouds, the retrieval of ozone from satellite measurements becomes more complicated. In order to have a better understanding of the effects of clouds on backscattered UV radiation observed from satellites, we need first to identify measurements from different types of cloudy scenes. Having separated measurements among different scenes, we can investigate the effects of clouds on backscattered UV radiation. In this paper we present a method to identify cloudy scenes from SBUV satellite measurements. Then the effects of horizontally extended clouds on the backscattered UV radiation are examined on the basis of observations and radiative transfer theory.

Data Description

The SBUV instrument on the Nimbus 7 satellite consisted of a double Ebert-Fastie spectrometer and a filter photometer flying at an altitude near 1200 km. The continuous mode of the spectrometer scans the Earth's backscattered spectrum from 160 nm to 400 nm, sampling data in 0.2-nm increments with a 1.1-nm half width triangular band pass. One complete spectral scan requires approximately 3 min. The photometer measures radiation at 343.3 nm with a 3-nm-wide band pass at a rate of once per second. Both spectrometer and photometer simultaneously view identical fields in the nadir direction taking measurements of the vertical component of backscattered solar UV radiation. The instantaneous angular field of view is 11.33° × 11.33° for both instruments, and this square moves at a speed of about 6.4 km/s [*Heath et al.*, 1978; *Schlesinger et al.*, 1988].

Paper number 95JD01753.
0148-0227/95/95JD-01753$05.00

Spectral Dependence of Backscattered UV Radiation

This section examines some features of the spectral scan measurements from SBUV. Since the SBUV sensor measures radiance in the vertical direction escaping from the atmosphere, a directional unitless spectral albedo may be defined as

$$A(w) = \pi I(w, \mu_0, \mu = 1)/[\mu_0 F_0(w)] \quad (1)$$

where the vertical radiance is $I(w, \mu_0, \mu = 1)$, $F_0(w)$ is the solar irradiance at wavelength w, μ is the cosine of the polar angle, and μ_0 is the cosine of the solar zenith angle. The factor π is introduced so that in the special case of a hemispherically isotropic backscattered radiance at the top of the atmosphere, $A(w)$ is the real albedo.

Figure 1 shows several spectral scan measurements for wavelengths greater than 280 nm. The spectral albedo increases with wavelength from 280 nm to 340 nm, with considerable variability. The spectral structure associated with the Huggins bands of ozone is evident. Beyond 340 nm the spectral albedos behave irregularly. The spectral albedo may increase or decrease for different scans in different wavelength regions.

It is apparent that spectral albedos vary from one scan to another. However, the spectral albedos can be sorted into two groups. One group of spectral albedos generally has small values characterized by an increase of albedo with wavelength, superimposed with the Huggins structure, reaching a maximum at about 340 nm, then decreasing gradually with wavelength. With relative small spectral albedos in general, this group of measurements represents clear scenes.

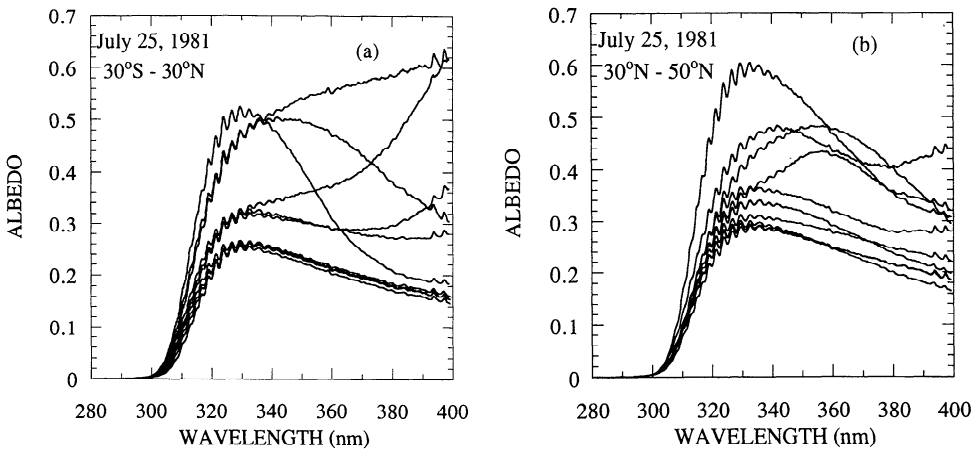

Figure 1. SBUV spectral albedos observed on July 25, 1981, in the latitude bands (a) 30°S to 30°N and (b) 30°–50°N. Scans with small values of albedo which gradually decrease for wavelengths longer than 340 nm represent homogeneous atmospheres; large values of albedo with irregular variations beyond 340 nm represent inhomogeneous atmospheres.

The spectral dependence of the albedo arises from competition between absorption by ozone and molecular scattering. Most ozone molecules reside in the stratosphere with a maximum concentration at about 25 km in the tropics and middle latitudes and at about 18 km in the polar region. However, the concentration of Rayleigh scatterers, molecular nitrogen and oxygen, decreases exponentially with height. About 80% of the molecules are concentrated in the troposphere. For short wavelengths, most of the UV radiation is absorbed by ozone before reaching the troposphere; hence a small amount of the UV radiation is scattered back to space and to the instrument. As wavelength increases, the ozone absorption cross section decreases and more photons reach the lower altitudes, where they experience more backscattering and hence escape to space. However, as wavelength increases and more photons reach the troposphere, Rayleigh scattering becomes dominant. Because the Raleigh cross section is inversely proportional to the fourth power of wavelength, the backscattered UV radiation is expected to decrease with wavelength beyond a certain point.

The other category of spectral scan measurements has larger albedos in general. For wavelengths shorter than about 335 nm, the spectral albedo increases with wavelength in a way similar to that for the first category. The characteristic feature of this group of scans is the irregular variation of spectral albedos for wavelength longer than 335 nm. Some measurements have very large albedos at the peak (about 335 nm) and then decrease sharply, while others show a continuous increase in spectral albedo or display large variability for wavelengths greater than 335 nm.

The anomalous spectral dependence is probably associated with the presence of tropospheric clouds in the field of view (FOV) of the instrument. As the satellite moves from cloudy to clear conditions, or from optically thick to optically thin clouds, the spectral albedos are expected to decrease sharply beyond a certain wavelength. Alternately, the spectral albedos will increase as the satellite flies from clear to cloudy conditions, or from optically thin to optically thick clouds. The changes in cloud cover or cloud optical depth in the FOV of the spectrometer are responsible for the irregular variation of observed spectral albedos. The shape of the spectral albedo at wavelengths greater than 335 nm is largely related to the cloud field.

Spatial Variations in Photometer Measurements and Correlations With Spectral Data

With negligible ozone absorption at 343.3 nm, the photometer measurements can be used to identify surface properties and clouds. For a clear atmosphere, both the absolute values and the spatial variations of the photometer measurements are expected to be small. Because photometer measurements vary continuously from a clear atmosphere to a cloudy atmosphere, the cutoff value between clear and cloudy atmospheres can be uncertain. Large spatial variations in the photometer measurements are expected for cloudy atmospheres with large horizontal variability. However, the photometer measurements over homogeneous layer clouds such as stratus and cirrus may display small spatial variability.

As the satellite flies, the footprint moves about 6.4 km during each consecutive photometer measurement. In the course of an entire spectral scan, the footprint moves about 600 km, and it is likely that changes in photometer albedos due to the presence of clouds or the changes in surface albedo will appear. However, during a smaller number of photometer measurements, more homogeneous scenes are expected. Figure 2 shows the relationship between the average albedo of 16 consecutive photometer measurements and the homogeneity of the scene, represented by the standard deviations of the 16 photometer albedos from the means. It is evident from Figure 2 that a homogeneous scene is associated with small photometer albedos at 343.3 nm. However, the distribution of the photometer albedo varies continuously, as is shown by Figure 3. It is not clear where to draw the line with one side homogeneous and other side inhomogeneous based only on the photometer albedo at 343.3 nm. Furthermore, homogeneous scenes with small standard deviations are also found with large photometer albedos. Those measurements should refer to horizontally extended cloudy scenes.

Figure 4 plots the measured albedos at specific wavelengths from a spectral scan versus the corresponding photometer al-

bedo. Albedos at 292 nm show little correlation with the photometer measurements, as one would expect given the strength of absorption at short wavelengths. The correlation improves as wavelength increases, until at 330 nm the albedo provides information that is redundant with the photometer. For subsequent analysis the spectral albedos from 290 nm to 330 nm are considered to arise from a homogeneous atmosphere if the standard deviation of the corresponding 16 photometer albedos is less than 0.005. Then histograms of data from homogeneous scenes are constructed to separate clear conditions from atmospheres with horizontally homogeneous clouds. We take the photometer albedo at the peak of the histogram as the cutoff between clear and cloudy conditions.

Effects of Horizontally Homogeneous Clouds on Backscattered UV Radiation

Observations

Clouds form on different horizontal scales and vertical extensions. Because of the large spatial coverage, stratiform clouds, such as cirrus anvil clouds and stratus clouds, may have large effects on the backscattered UV radiation. Clouds of this kind have less spatial variation in optical properties than do cumulus clouds. Hence in these cases the backscattered UV radiation may be modeled properly with the plane parallel approximation. To gain physical insight into how clouds affect the backscattered UV radiation, we focus on the effects of horizontally homogeneous clouds. Since very little UV radiation can be sensed at wavelengths shorter than 290 nm and the ozone absorption cross section is very small for wavelengths longer than 330 nm, we consider only the wavelength region between 290 nm and 330 nm.

Besides clouds, the backscattered UV radiation can be affected by the ozone amount and the solar zenith angle. In order to minimize other factors, we examined the relative difference between backscattered UV albedos from homogeneous cloudy scenes and those from clear scenes for the tropical region and higher latitudes. Figure 5 presents examples for different latitudes. The enhancement of spectral albedo may be defined as the relative difference between the cloudy atmosphere albedo and the albedo from a clear atmosphere, given as

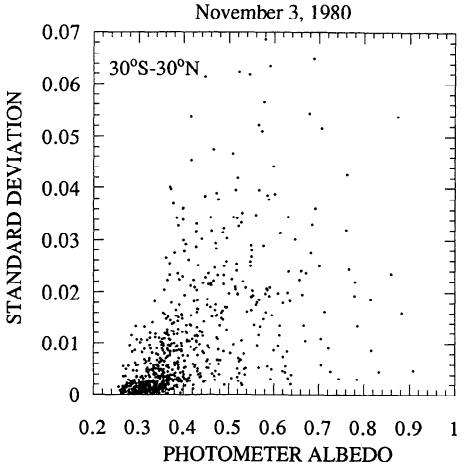

Figure 2. Scatterplot of averaged photometer albedo based on every consecutive 16 measurements and the related standard deviation from 30°S to 30°N, November 3, 1980.

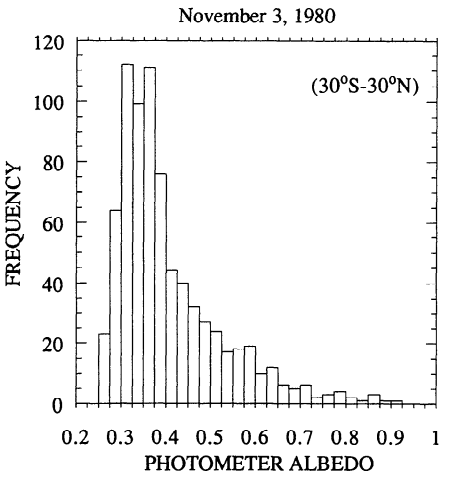

Figure 3. Frequency distribution of the averaged photometer albedo for the data shown in Figure 2.

$$\text{Enhancement} = [\text{Albedo(cloudy)} - \text{Albedo(clear)}]/\text{Albedo(clear)} \quad (2)$$

The enhancement of spectral albedo appears at certain minimum wavelengths and then generally increases with wavelength. However, the enhancements exhibit some special features. For some observations in the tropical region, the enhancements increase rapidly from wavelengths of about 296 nm to 305 nm, then slowly increase toward longer wavelengths. The enhancements could reach to 1.7 times the value for a clear atmosphere. The enhancements at midlatitudes are smaller than those in the tropical region at short wavelengths.

The two characteristic features of the enhancements are probably related to different types of clouds. Since only horizontally homogeneous clouds are concerned, the height of the clouds and optical depth should be the two major factors that could affect the backscattered UV radiation as shown in Figure 5. In the following section, we present a series of radiative transfer calculation to interpret the observations.

Numerical Analysis

Model description. In order to investigate the effects of clouds on the backscattered UV radiation in more detail, a series of calculations were performed using a discrete ordinates radiative transfer model [*Stamnes et al.*, 1988]. For given solar zenith angle, optical depth, phase function, and single-scattering albedo, the model solves the radiative transfer equation numerically for a vertically inhomogeneous atmosphere. The U.S. Standard Atmosphere is used for the vertical profile of molecular number density. The Rayleigh scattering cross sections are taken from *World Meteorological Organization* [1985]. The ozone absorption cross sections [*Molina and Molina*, 1986] are used to calculate ozone extinction in the model. For a given total ozone amount, statistical relations [*Bojkov*, 1969] are applied to estimate the vertical profile.

The atmosphere and clouds are assumed to be plane parallel with a Lambertian reflecting surface underneath. Homogeneous optical properties (e.g., phase function, single-scattering albedo) are assumed within the cloud. For water clouds, the phase function depends on the size distribution of cloud droplets. We have examined the optical properties of two distinctive water clouds in the ultraviolet spectral region. The clouds are

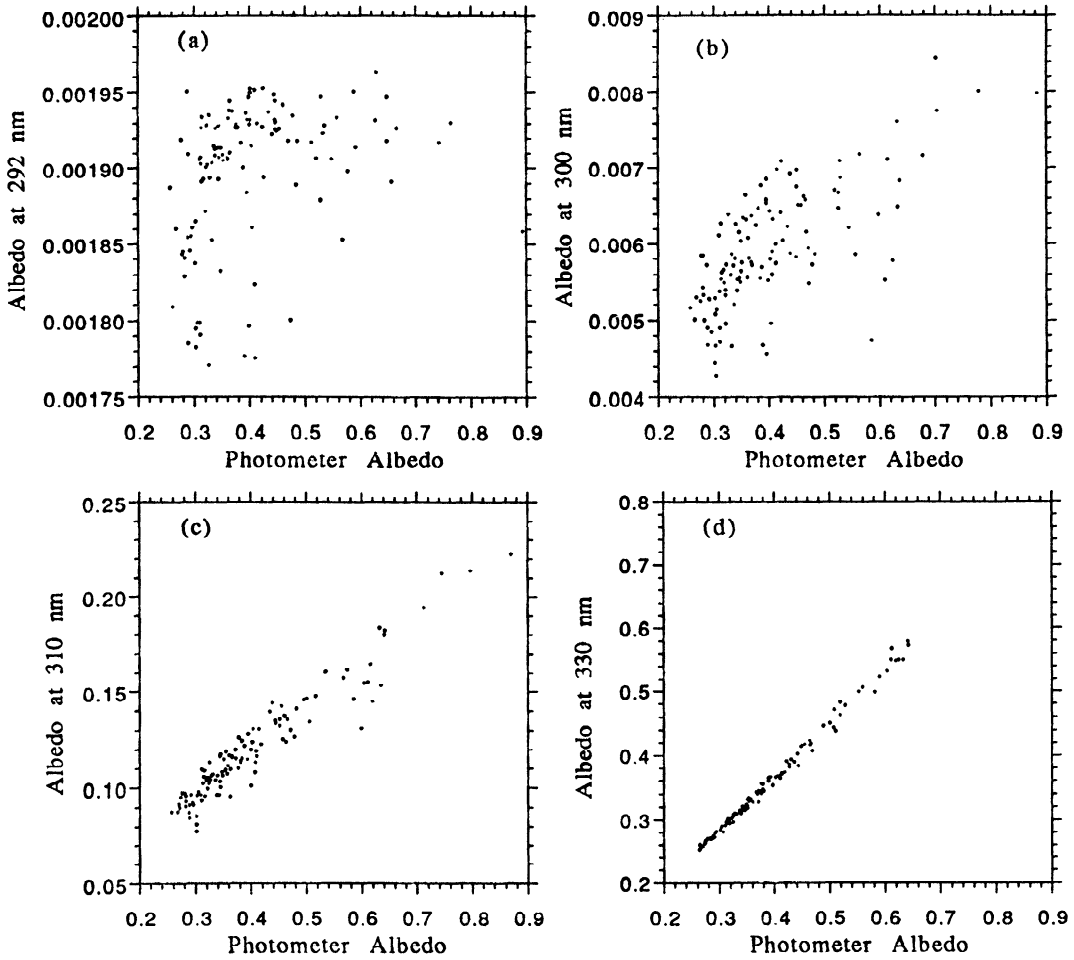

Figure 4. Relationship between the spectral albedo at selected wavelengths and the corresponding photometer albedo at 343.3 nm, for wavelengths of (a) 292 nm, (b) 300 nm, (c) 310 nm, and (d) 330 nm.

assumed to consist of typical modified gamma distributions [*Hansen*, 1971] with mean effective radii of 5.56 μm and 11.19 μm and effective variances of 0.111, and 0.193 respectively. The two clouds may represent extremes of the wide range of cloud size distributions. Mie theory was used to calculate the phase function of the two water clouds [*Bohren and Huffman*, 1983]. Figure 6 shows that the phase functions of the two clouds resemble one another to a large degree.

Figure 7 presents the albedos computed for both phase functions versus cloud optical depth. Results appear for solar

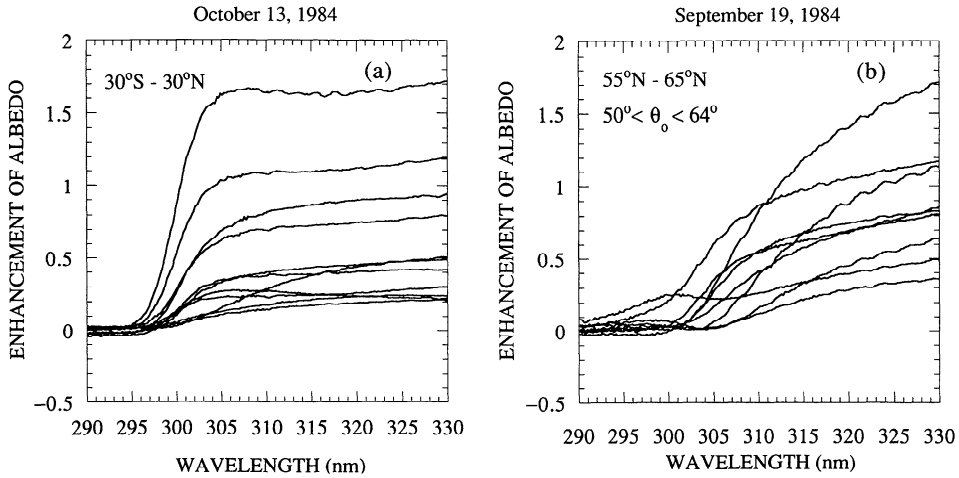

Figure 5. (a) Enhancement of spectral albedo in the tropical region (30°N to 30°S) on October 13, 1984. (b) Enhancement of spectral albedo in the latitude band 55°–65°N, with solar zenith angle between 50° and 64°, on September 19, 1984.

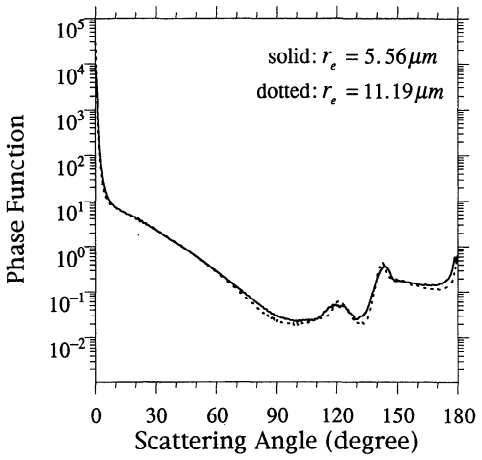

Figure 6. Phase functions for two clouds whose drop sizes are described by the modified gamma distribution at wavelength of 0.3 μm with refractive index $1.34 + 1.6 \times 10^{-8}i$. The solid curve is for a mean effective radius r of 0.56 μm and effective variance of 0.111 ($0.05\ \mu m < r < 12\ \mu m$); the dotted curve is for r of 11.19 μm and effective variance of 0.193 ($0.05\ \mu m < r < 20\ \mu m$).

zenith angles of 5° (Figure 8a) and 60° (Figure 8b). Despite the different phase functions, the clouds have very similar effects on backscattered UV radiation. Since we do not attempt to retrieve detailed optical properties in this study, the average of the phase functions of the two clouds is used. The averaged phase function of the two extreme size distributions would appropriately represent the phase function of water clouds having a wide range of size distributions.

The radiative properties of ice clouds are more complicated than the cases considered above. The scattering properties of ice clouds depend on the size distribution, shape, and orientation of ice particles. Difficulties are often encountered in performing radiative transfer calculations in ice clouds due to lack of observations of the size distribution and orientation of ice particles, and complications of treating an anisotropic medium. The phase function of water clouds certainly differs from those of ice clouds. However, one may expect that the discrepancy in the computed backscattered UV radiance by using the water cloud phase function will be compensated by increasing or decreasing optical depth of clouds.

Numerical results. Since the backscattered UV radiation depends not only on cloud properties but also on ozone amount and solar zenith angle, the radiative transfer calculations were carried out for total ozone amounts of 280 Dobson units (DU) and 350 DU representing tropical and mid-latitude conditions, for solar zenith angles of 0° and 60° respectively. Clouds at altitudes of 1–2 km and 4–6 km are considered to represent low and middle level clouds. High clouds are assumed to be at 14–16 km for the tropical region and 8–10 km for mid-latitudes. The spectral albedos from the cloudy atmosphere are compared with those from the clear atmosphere. The enhancements of the albedo due to clouds are shown in Figures 8 and 9.

Similar to the satellite observations, the enhancements appear at certain wavelengths and then generally increase with wavelength. For any given cloud optical depth, the increase of the enhancement with increasing wavelength arises from the decrease in absorption of UV radiation by ozone. Radiation at wavelength less than 290 nm is primarily absorbed in the stratosphere before entering the troposphere. As wavelength increases, more UV radiation can penetrate to the troposphere. Hence UV radiation at longer wavelengths may be affected by tropospheric clouds. Structure in the Huggins bands of ozone appears in the enhancements, and enhancements are more pronounced for optically thicker clouds than optically thinner clouds. The magnitude of this structure is larger for low clouds than for high clouds. It is also interesting to note that there are no clear Huggins bands structures in the enhancements computed for high clouds (8–10 km) at midlatitudes.

Clouds located at different altitudes lead to substantial differences in the enhancements of spectral albedo. The enhancements of backscattered UV radiation appear at shorter wavelengths for high clouds than for low clouds. Compared with low clouds, high clouds are found to be more efficient at enhancing backscattered UV radiation at short wavelengths. For an overhead Sun the enhancements at a wavelength of 300 nm from high clouds (14–16 km) are about 5 times those from low

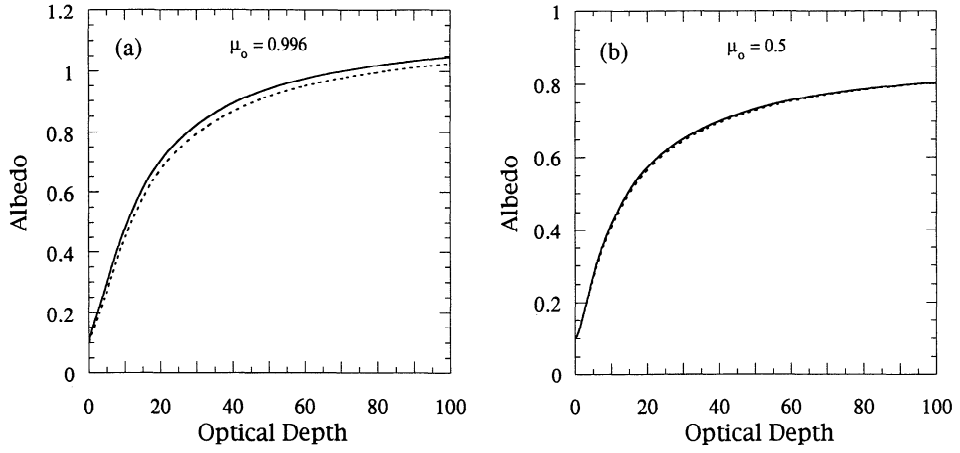

Figure 7. Dependence of backscattered albedo on cloud optical thickness computed for the two phase functions in Figure 7 at the wavelength of the photometer, for solar zenith angle of (a) approximately 5° and (b) 60°. The solid curves refer to a mean effective cloud drop radius of 5.56 μm, and the dashed curves refer to a radius of 11.19 μm.

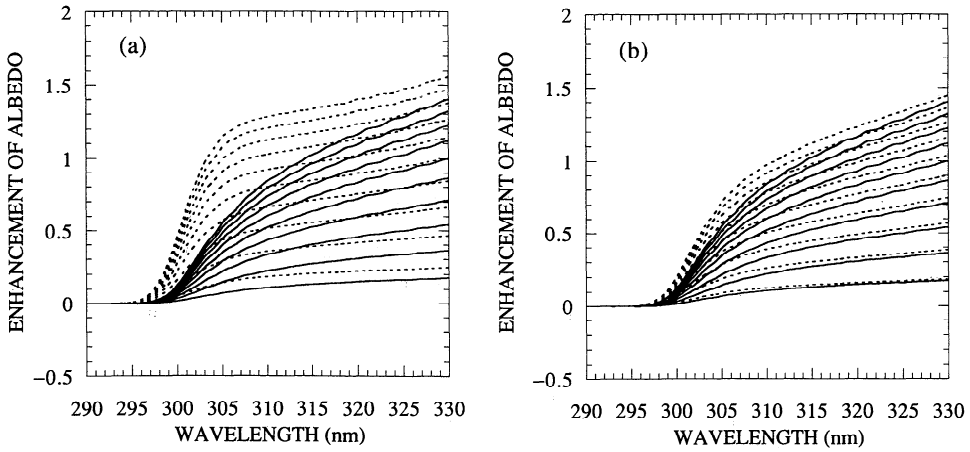

Figure 8. The enhancement of spectral albedo based on calculations with total ozone of 280 DU, cosine of solar zenith angle of 1.0, and optical depths of 2, 4, 6, . . . , 20 from lower to upper curves. (a) The solid curves represent enhancements associated with low level clouds (1–2 km), and the dotted curves are enhancements from high clouds (14–16 km). (b) The solid curves are the same as in Figure 8a; the dotted curves are enhancements associated with middle level clouds (4–6 km).

clouds (1–2 km) with the same optical depths (Figure 8a). For a solar zenith angle of 60° the enhancements of UV radiation at 305 nm from high clouds (8–10 km) are about double those from low clouds (1–2 km) with the same optical depth (Figure 9a). Middle level clouds are more efficient than low clouds at enhancing backscattered UV radiation at short wavelengths (Figures 8b and 9b). However, high clouds, especially in the tropical region, are far more efficient in enhancing the backscattered UV radiation at short wavelengths than are middle and low level clouds. The efficiency of high clouds in backscattering UV radiation at short wavelengths is related to the fact that photons experience more scattering and absorption when clouds are at lower altitudes. The absorption tends to decrease the backscattered UV radiation, while molecular scattering acts in the opposite sense. The net effect is the result of this competition.

Because the ozone absorption cross section increases rapidly toward shorter wavelengths, absorption would be dominant over molecular scattering at short wavelengths. Because of tropospheric ozone absorption, there are fewer photons at short wavelengths reaching the low clouds as compared with high clouds. Hence, it is expected that low clouds will be much less efficient than high clouds in backscattering UV radiation at short wavelengths. The differences between the enhancements of spectral albedo from high clouds and those from low clouds will be small at longer wavelengths.

The enhancement of the backscattered UV radiation depends on cloud height and optical depth, the total ozone amount, ozone profile, surface albedo, and solar zenith angle. However, radiative transfer modeling shows that the spectral dependence of the enhancement primarily depends on the height of the clouds. By comparing the observations with modeled results, it is likely that the enhancements in Figure 5a are from cirrus clouds in the tropics. The enhancements in Figure 5b are more complicated. Those with Huggins band structure are likely related to low or middle level clouds, while the one without this structure and with larger enhancements is probably from high clouds.

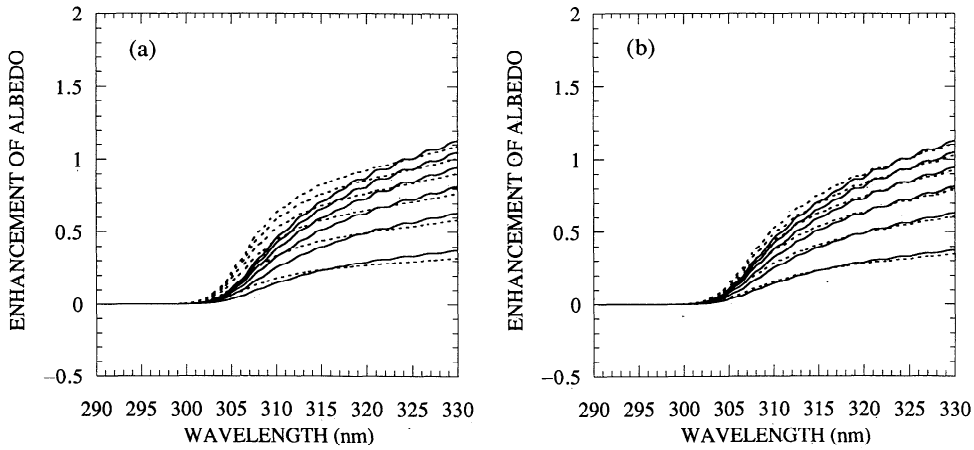

Figure 9. (a) The enhancement of spectral albedo based on radiative transfer calculations with total ozone of 350 DU, cosine of solar zenith angle of 0.5, and optical depths of 5, 15, 20, 25, and 30 from lower to upper curves. The solid curves represent enhancements associated with low level clouds (1–2 km), and the dotted curves are enhancements from high clouds (8–10 km). (b) The solid same curves are the same as in Figure 9a, the dotted curves are enhancements associated with middle level clouds (4–6 km).

Summary

In this study we have examined the effects of horizontally extended clouds on the backscattered UV radiation using satellite observations and radiative transfer modeling. The enhancements of spectral albedo appear as of certain minimum wavelengths in both the observed and modeled results. The enhancements generally increase with wavelength. However, the numerical results show that low clouds and high clouds behave differently. The enhancements associated with high clouds are generally larger than those due to low clouds at short wavelengths. For the same optical depth, the enhancements related to high clouds are about 5 times those due to low clouds at a wavelength 300 nm in the tropical region and an overhead Sun. At mid-latitudes, high clouds are twice as effective as low clouds in backscattering UV radiation at the wavelength 305 nm and a solar zenith angle of 60°.

High clouds are responsible for the observed enhancements of backscattered albedo in the tropical region, while low clouds are more often related to the enhancements at midlatitudes. The cirrus anvil clouds in the tropics and stratiform clouds at midlatitudes are the two most likely horizontally extended clouds to produce the observed enhancements in backscattered albedo. Since high clouds and low clouds differ greatly from one another in backscattering UV radiation, especially at short wavelengths where absorption is significant, the two types of clouds should be treated separately in ozone retrievals.

Acknowledgments. Portions of this work were supported by the National Aeronautics and Space Administration under grant NAG5-873.

References

Bohren, C. F., and D. R. Huffman, *Absorption and Scattering of Light by Small Particles*, John Wiley, New York, 1983.

Bojkov, R. D., Computing the vertical ozone distribution from its relationship with total ozone amount, *J. Appl. Meteorol.*, *8*, 284–292, 1969.

Frederick, J. E., and D. Lubin, The budget of biologically active solar ultraviolet radiation in the Earth-atmosphere system, *J. Geophys. Res.*, *93*, 3825–3823, 1988.

Hansen, J. E., Multiple scattering of polarized light in planetary atmosphere, II, Sunlight reflected by terrestrial water clouds, *J. Atmos. Sci.*, *28*, 1400–1426, 1971.

Heath, D., A. J. Krueger, and H. Park, The solar backscatter ultraviolet (SBUV) and total ozone mapping spectrometer (TOMS) experiment, in *The Nimbus 7 User's Guide*, pp. 175–211, NASA Goddard Space Flight Center, Greenbelt, Md., 1978.

Molina. L. T., and M. J. Molina, Absolute absorption cross section of ozone in the 185- to 350-nm wavelength range, *J. Geophys. Res.*, *91*, 14,501–14,508, 1986.

Stamnes, K., S. Tsay, W. Wiscombe, and K. Jayaweera, Numerically stable algorithm for discrete ordinate-method radiative transfer in multiple scattering and emitting layered media, *Appl. Opt.*, *27*, 2502–2509, 1988.

Schlesinger, B. M., R. P. Cebula, D. F. Heath, and A. J. Fleig, Nimbus 7 solar backscatter ultraviolet (SBUV) spectral scan Solar irradiance and Earth radiance product user's guide, *NASA Ref. Publ.*, RP-1199, 5–24, 1988.

Wen, G., and J. E. Frederick, Ozone within the El Chichón aerosol cloud inferred from solar backscatter ultraviolet continuous-scan measurements, *J. Geophys. Res.*, *99*, 1263–1271, 1994.

World Meteorological Organization, Atmospheric ozone 1985, *Rep. 16*, 908 pp., Global Ozone Res. and Monit. Proj., Geneva, 1985.

J. E. Frederick and G. Wen, Department of the Geophysical Sciences, University of Chicago, 5734 South Ellis Avenue, Chicago, IL 60637.

(Received August 22, 1994; revised March 15, 1995; accepted March 24, 1995.)